Journal of Biomechanics 43 (2010) 1310–1315

Contents lists available at ScienceDirect

Journal of Biomechanics

journal homepage: www.elsevier.com/locate/jbiomech
www.JBiomech.com

Material and surface factors influencing backside fretting wear in total knee replacement tibial components

Fabrizio Billi [a], Sophia N. Sangiorgio [a], Sarah Aust [b], Edward Ebramzadeh [a,*]

[a] The J. Vernon Luck, Sr. Orthopaedic Research Center, Los Angeles Orthopaedic Hospital/UCLA, 2400 South Flower Street, Los Angeles, CA 90007, USA
[b] Depuy Orthopaedics, 700 Orthopaedic Drive, Warsaw, IN 46581-0988, USA

ARTICLE INFO

Article history:
Accepted 25 January 2010

Keywords:
Fretting
Micromotion
Surface roughness
Knee replacement
Polyethylene
Titanium alloy
Cobalt alloy

ABSTRACT

Retrieval studies have shown that the interface between the ultra-high molecular weight polyethylene insert and metal tibial tray of fixed-bearing total knee replacement components can be a source of substantial amounts of wear debris due to fretting micromotion. We assessed fretting wear of polyethylene against metal as a function of metal surface finish, alloy, and micromotion amplitude, using a three-station pin-on-disc fretting wear simulator. Overall, the greatest reduction in polyethylene wear was achieved by highly polishing the metal surface. For example, highly polished titanium alloy surfaces produced nearly 20 times less polyethylene wear compared with blasted titanium alloy, whereas, decreasing the micromotion amplitude from 200 to 50 μm produced approximately four times less polyethylene wear for the same blasted titanium alloy surface. Although the effect of the metal alloy was much smaller than the effect of metal surface roughness or the micromotion amplitude, CoCr discs produced slightly greater polyethylene fretting wear than titanium alloy discs under each condition. The results are essential in design and manufacturing decisions related to fixed-bearing total knee replacements.

1. Introduction

Particulate wear debris from implants is largely recognized as a major cause of bone resorption and osteolysis, representing one of the leading reasons of clinical failure of total joint replacements. Recently, there has been increasing awareness that, in addition to articulating surfaces, non-articulating surfaces, such as implant fixation interfaces and modular component junctions, can generate substantial amounts of debris as a result of micromotion and fretting wear. In total knee replacements, fretting between the backside of the ultra-high molecular weight polyethylene insert and the tibial tray of fixed bearing tibial components is documented to generate significant amounts of polyethylene debris. Although difficult to quantify, some studies have estimated polyethylene from the backside of the tibial tray alone to wear an average of 100–138 mm^3 per year (Conditt et al., 2005; Li et al., 2002). These investigators have further noted that such rates were comparable to runaway wear from the articular surfaces of severely wearing polyethylene acetabular components in total hip replacements, and capable of originating clinically significant levels of bone resorption.

The importance of fretting in knee replacements has led to redesigning locking mechanisms, reducing micromotion. However, the relative influences of metal surface roughness, alloy, and micromotion on fretting wear have not been systematically studied. Rather, most studies have used retrieved implants, scoring damage on the inferior surface (Engh et al., 2001; Harman et al., 2007; Rao et al., 2002; Surace et al., 2002; Wasielewski et al., 1997), measuring polyethylene extrusion from inferior insert surfaces into tibial tray screw holes (Conditt et al., 2005), or measuring decreases in depths of manufacturer's stamped markings on the inferior polyethylene surface (Crowninshield et al., 2006). Although these studies provide valuable information, they are indirect retrospective measurements.

Variables affecting backside interface micromotion and the resultant wear (Conditt et al., 2004b) include metal surface finish, alloy, implant design, and locking mechanism. Retrieval studies have not isolated or quantified individual influences of variables on backside wear, as they cannot systematically control independent variables. Wear simulator studies inherently include the complexities of implant design, locking mechanism, and other variables, again, making it difficult to isolate the effects of individual variables, or even to separate backside wear from articular surface wear without additional indirect measurements (Muratoglu et al., 2007).

In this study, we used a crossing-path fretting wear simulator to measure the relative effects of metal surface finish, alloy, and

* Corresponding author. Tel.: +1 213 742 1378; fax: +1 213 742 1384.
E-mail address: ebramzad@usc.edu (E. Ebramzadeh).

0021-9290/$ - see front matter © 2010 Elsevier Ltd. All rights reserved.
doi:10.1016/j.jbiomech.2010.01.015

micromotion amplitude, representative of those on the backside of tibial components, on fretting wear behavior of polyethylene against metal, under simulated physiological conditions.

2. Materials and methods

2.1. Simulator

The three-station simulator generated fretting wear by creating small tangential micromotion between pins and discs. Mounted in an MTS 812 servohydraulic load frame (MTS Corporation, Minneapolis, MN), it consisted of three pin-on-disc assemblies each in a chamber of 90% bovine serum (Fig. 1). Discs were mounted on the base plate, while each pin was mounted at the end of an L-shaped structure, 165 mm from its corresponding vertical rod.

Cyclic axial load was applied through a central ball joint. Fretting micromotion combined rotational and linear motions, producing crossing-path motion. Linear motion was produced using the deformation of the three vertical rods under bending (Fig. 1; Ebramzadeh et al., 2005). A four-bar linkage generated rotational micromotion (Fig. 1).

2.2. Experimental variables

Pins (10 mm diameter) were made of ultra-high molecular weight polyethylene, gamma sterilized in foil barrier packaging under vacuum. Metal discs were made of titanium alloy (Ti–6Al–4V) or cobalt chromium alloy, with highly polished or blasted surfaces (Table 1). The blasted surfaces for both titanium alloy and cobalt chromium alloy discs had a nominal R_a of 2 μm. In contrast, the polishing treatment produced a somewhat smaller R_a for the CoCr alloy (0.05) than for the titanium alloy (0.2). Both the blasted and polished surface finishes were typical of tibial tray surfaces of implants that have been in wide clinical use. Combining surface finish (blasted or polished), disc material, and fretting micromotion, a total of eight experiments were conducted. Each experiment consisted of six pin-on-disc pairs—three were fretted and three were load-soak controls. Controls were also tested in serum, undergoing axial loading only (Fig. 1). Weight changes of controls were used to correct for water absorption. Similarly, dimensional changes of controls were subtracted from height loss measurements to correct for creep deformation.

Linear motion amplitudes were based on Engh et al. (2001), who measured a mean of 64 μm of tibial insert motion in several designs of modular fixed-bearing TKRs and as much as 380 μm in autopsy retrieved components. Similarly, Rao et al. (2002) measured between 106 and 760 μm of insert motion in vitro. Conditt et al. (2004a) showed that axial compressive gait forces on the insert reduced mean insert motion from 618 to 103 μm. Therefore, for the present study, rotational motion amplitude of 3° (i.e., $\pm 1.5°$) was combined with linear motion amplitude of 50 or 200 μm.

Crossing-path motion was determined by calculating the trajectory of each point on the pin relative to the disc under linear pin and angular disc motions. The trajectory of each point was a combination of two harmonic linear and rotational (along an arc) motions. Rotation was about the central pin axis; consequently, the pin center experienced only linear motion (50 or 200 μm). In contrast, points at the pin edge underwent circumferential motion of 130 μm. Rotational motion increased linearly moving away from the pin center. Total sliding distances were estimated by averaging the sliding distance of the 360 points for each cycle and multiplying by 5 million cycles (5 years' use). An oscillation of $\pm 1.5°$ was determined to optimize the crossing-path trajectory with linear motion amplitudes.

An axial double-peak Paul-curve load profile was applied. To determine the maximum compressive stress at the contact surface, in vivo tibial insert contact stresses were needed. Villa et al. (2004) conducted an extensive study to measure and calculate contact pressures on the front (superior) and backside (inferior) of rotating hinge tibial inserts under varying flexion degrees. While their models were based on a rotating hinge design, their measurements and computational model were both static and therefore provided a reasonable estimate of contact stresses in any similar design, including fixed bearing designs. They reported peak backside stresses of approximately 10 MPa. The load in the present study applied peak stresses of 10 MPa, at 3 Hz.

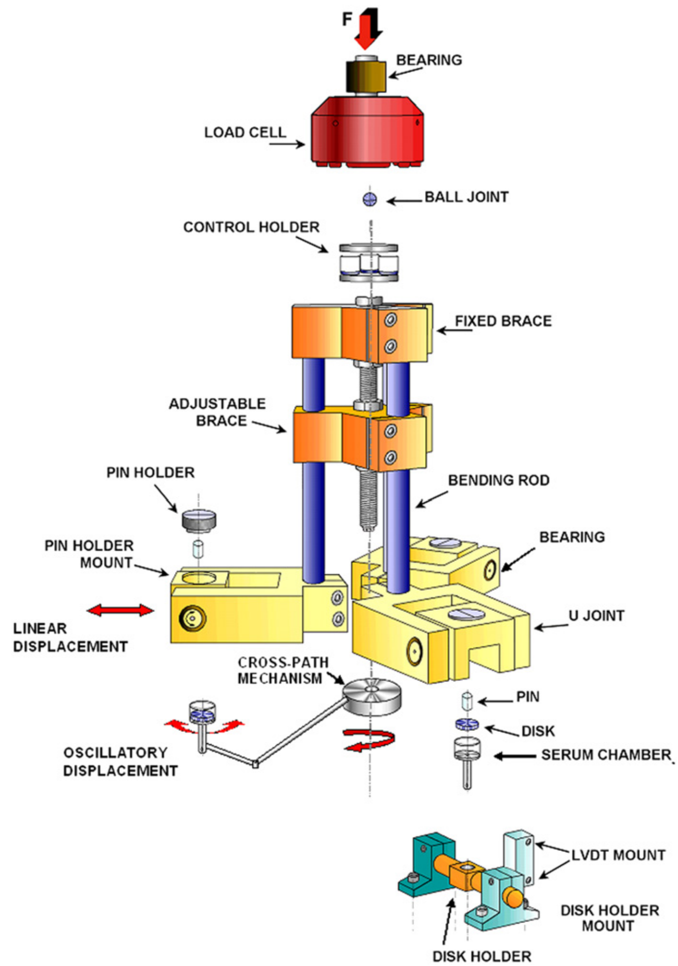

Fig. 1. Three-station pin-on-disc fretting wear simulator.

Table 1
Experimental design and the resultant polyethylene fretting wear rates are shown. The independent variables were metal disc alloy, metal surface roughness, and fretting motion amplitude. The outcome, polyethylene wear, was measured by both dimensional and gravimetric analysis.

Metal		Fretting motion amplitude (μm)	Polyethylene	
Metal disc alloy	Surface finish		Wear rate, dimensional/ CMM (mm^3/million cycles)	Wear rate calculated from weight loss (mm^3/million cycles)
Ti–6Al–4V	Polished, R_a=0.20, R_{sk}=−1.3	50	-0.02 ± 0.01	-0.001 ± 0.01
Ti–6Al–4V	Polished, R_a=0.19, R_{sk}=−1.4	200	0.09 ± 0.02	0.09 ± 0.01
Ti-6Al-4 V	Blasted, R_a=1.9, R_{sk}=−2.1	50	0.38 ± 0.31	0.59 ± 0.43
Ti–6Al–4V	Blasted, R_a=1.9, R_{sk}=−2.1	200	1.50 ± 0.85	2.88 ± 0.10
CoCrMo alloy	Polished, R_a=0.05, R_{sk}=−6.7	50	0.12 ± 0.1	-0.18 ± 0.01
CoCrMo alloy	Polished, R_a=0.05, R_{sk}=−6.7	200	0.2 ± 0.05	0.44 ± 1.11
CoCrMo alloy	Blasted, R_a=2.0, R_{sk}=−1.3	50	0.53 ± 0.12	0.63 ± 0.01
CoCrMo alloy	Blasted, R_a=1.9, R_{sk}=−1.1	200	1.63 ± 0.86	2.88 ± 1.10